The electrical properties of polycrystalline silicon films

John Y. W. Seto

Citation: Journal of Applied Physics **46**, 5247 (1975); doi: 10.1063/1.321593
View online: http://dx.doi.org/10.1063/1.321593
View Table of Contents: http://scitation.aip.org/content/aip/journal/jap/46/12?ver=pdfcov
Published by the AIP Publishing

The electrical properties of polycrystalline silicon films

John Y. W. Seto

Electronics Department, GM Research Laboratories, Warren, Michigan 48090
(Received 14 July 1975)

Boron doses of 1×10^{12} - $5 \times 10^{15}/cm^2$ were implanted at 60 keV into 1-μm-thick polysilicon films. After annealing at 1100°C for 30 min, Hall and resistivity measurements were made over a temperature range -50–250°C. It was found that as a function of doping concentration, the Hall mobility showed a minimum at about $2 \times 10^{18}/cm^3$ doping. The electrical activation energy was found to be about half the energy gap value of single-crystalline silicon for lightly doped samples and decreased to less than 0.025 eV at a doping of $1 \times 10^{19}/cm^3$. The carrier concentration was very samll at doping levels below $5 \times 10^{17}/cm^3$ and increased rapidly as the doping concentration was increased. At $1 \times 10^{19}/cm^3$ doping, the carrier concentration was about 90% of the doping concentration. A grain-boundary model including the trapping states was proposed. Carrier concentration and mobility as a function of doping concentration and the mobility and resistivity as a function of temperature were calculated from the model. The theoretical and experimental results were compared. It was found that the trapping state density at the grain bound was $3.34 \times 10^{12}/cm^2$ located at 0.37 eV above the valence band edge.

PACS numbers: 73.60.F, 73.20.H, 72.20.F

INTRODUCTION

The electrical properties of polycrystalline silicon (polysilicon) films prepared by thermal decomposition of silane and doped by diffusion or during growth have been reported by various researchers.[1–4] In some of these experiments only the dopant-to-silicon atomic ratio in the gas phase was known. In others, the doping concentration was assumed to be the same as the carrier concentration of the epitaxial single-crystalline silicon prepared at the same time or under the same conditions. This appeared to be a reasonable assumption. However, there is still doubt as to what was the actual doping concentration. When experimental results are to be compared with theory, it is important that the impurity concentration be known precisely. In the present work, this is accomplished by using ion implantation. Hall measurements were reported by Kamins[4] and Cowher and Sedgwick[3] but their results were not in good agreement with each other. Neither Hall effect nor resistivity vs temperature have previously been measured or calculated for polysilicon films, although Muñoz *et al.*[5] performed such measurements on undoped bulk polysilicon rods.

Here we report the results of our electrical measurements on polysilicon films ion implanted with boron so that the doping concentration could be precisely controlled. We made Hall and resistivity measurements over a wide range of temperatures on polysilicon films doped from 1×10^{16} to $5 \times 10^{19}/cm^3$. A theoretical model is proposed and detailed calculations of the electrical transport properties of polysilicon are compared with experimental results.

EXPERIMENT

The polysilicon films were intentionally prepared undoped by thermal decomposition of silane in argon onto a layer of approximately 3000 Å of silicon dioxide which was thermally grown on p-type 10-Ω cm ⟨111⟩-oriented silicon wafers. All polysilicon depositions were done at 650°C in an infrared heated horizontal reactor. The details of the deposition procedure have been reported elsewhere.[6] The thickness of the polysilicon films used in this study ranged from 0.99 to 1.12 μm. Boron doses ranging from 1×10^{12} to $5 \times 10^{15}/cm^2$ were implanted into the polysilicon films at 60 keV energy. The samples were then annealed at 1100°C for 30 min in a dry nitrogen atmosphere. The annealing was intended to eliminate most of the damage produced by the implantation process and to create a uniform impurity distribution in the polysilicon films due to redistribution by diffusion. Hall measurements on successively anodized and stripped samples show that both carrier concentration and mobility were uniformly distributed. After annealing, Hall bar samples were delineated photolithographically. Aluminum was then electron-beam deposited and another photomask and etching was used to define the contacts. The contacts were alloyed at 500°C for 10

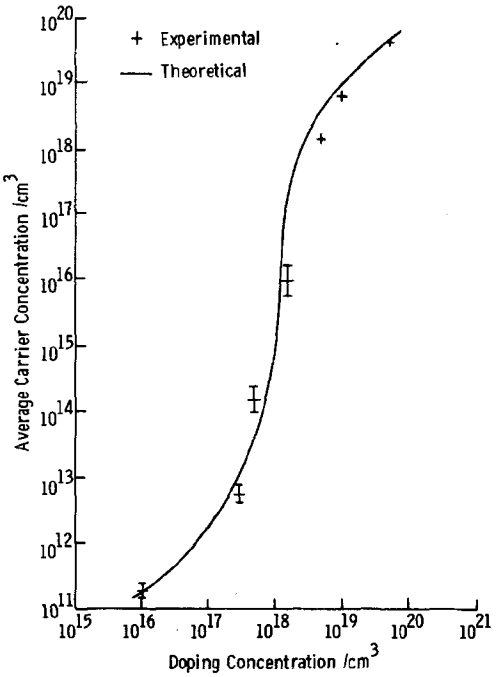

FIG. 1. Comparison of the calculated average carrier concentration vs doping concentration with the room-temperature Hall-measurement data. The solid line is the theoretical curve.

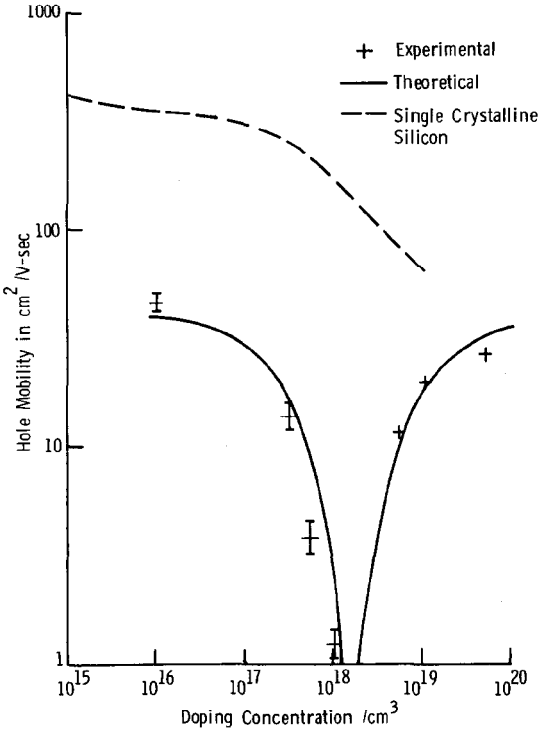

FIG. 2. Room-temperature hole Hall mobility vs doping concentration. The experimental result is plotted together with the theoretical solid curve. The broken line is for single-crystalline silicon.

min to make good Ohmic contacts. Hall measurements were made in magnetic inductions up to 1 T. Hall voltages were always found to be proportional to the applied magnetic field and current through the samples. For each measurement the current polarity was reversed and the Hall voltages in both directions were averaged for calculating the carrier concentration and mobility. In samples doped with less than $5\times10^{17}/cm^3$ of boron, the resistance across the Hall bar was over 10^7 Ω and could be as high as 10^{11} Ω. For those samples, the current was supplied by a specially built polyethylene isolated current supply. The Hall voltage was measured by a digital voltmeter buffered by a unity gain electrometer amplifier having an input impedance of 10^{14} Ω. When measuring the Hall coefficient and resistivity vs temperature, the sample was mounted on an aluminum block which was enclosed in an aluminum container. The temperature was measured by a thermocouple in direct contact with the back of the polysilicon sample. The whole setup was placed in a temperature chamber. The temperature variation during a measurement was less than ±0.5°C.

EXPERIMENTAL RESULTS

Figure 1 is a plot of the carrier concentration vs doping concentration. Since the carriers were found to be uniformly distributed in the film the doping concentration was obtained by dividing the total dose/cm^2 by the thickness of the polysilicon film. At a doping concentration of $10^{16}/cm^3$ the carrier concentration is only about $1.8\times10^{11}/cm^3$. As the doping concentration is increased, the carrier concentration remains very small compared to the doping concentration and then increases very rapidly when the doping concentration reaches about $5\times10^{17}/cm^3$. For a doping concentration of $5\times10^{18}/cm^3$ the carrier concentration is approximately 28% of the doping. As the doping concentration is increased further, the carrier concentration approaches that of the doping concentration. Our result is quite similar to that obtained by Cowher and Sedgwick[3] who doped their polysilicon films during growth.

The hole mobility in polysilicon and in single-crystalline silicon as a function of doping concentration are plotted in Fig. 2. The most prominent feature in Fig. 2 is the mobility minimum at a doping concentration slightly above $1\times10^{18}/cm^3$. As the doping is increased above $1\times10^{19}/cm^3$ the mobility approaches that in single-crystalline silicon. For doping less than $1\times10^{18}/cm^3$, the mobility increases as the doping is decreased but the mobility is always much smaller than that in single-crystalline silicon. Our over-all result is very much like that of Cowher and Sedgwick.[3] However, the mobility of their lightly doped samples was much higher, while the mobility of the heavily doped samples was smaller than this work. Figure 3 is a plot of the room-temperature resistivity as a function of doping. The resistivity reached 10^6 Ω cm for lightly doped samples. Increasing the doping from about $1\times10^{18}/cm^3$ results in an abrupt resistivity drop of about five orders of magnitude for only a factor of 10 further increase in doping concentration. Beyond that range the resistivity decreases almost linearly for further increase in doping. The abrupt decrease in resistivity is the result of the increase in carrier concentration and mobility as shown in Figs. 1 and 2.

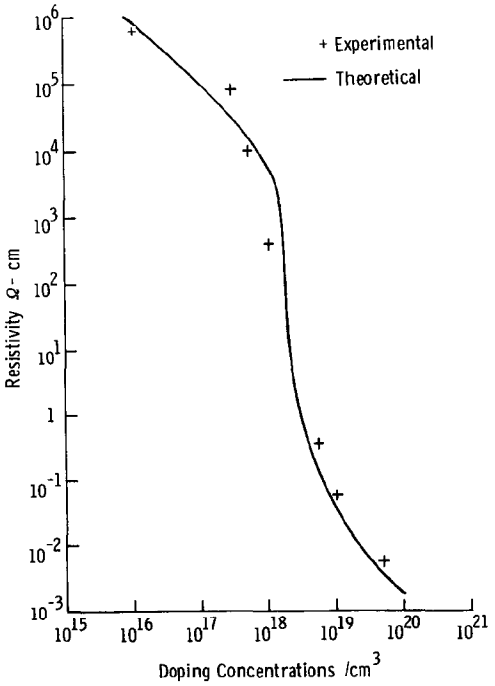

FIG. 3. Room-temperature resistivity vs doping concentration. The experimental data is plotted with theoretical curve.

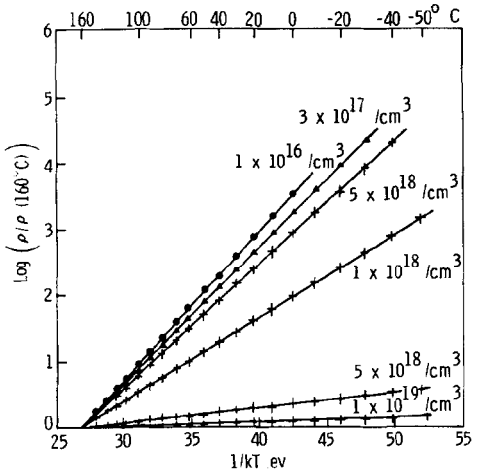

FIG. 4. Logarithm of resistivity vs $1/kT$ for samples with different doping concentrations. The resistivity is normalized by the resistivity at 160°C.

Figure 4 is a logarithmic plot of resistivity normalized by the resistivity at 160°C vs $1/kT$. A linear dependence on $1/kT$ is observed for all samples doped from 1×10^{16} to $1\times10^{19}/cm^3$. The slopes of the curves decrease as the doping was increased. The rate of decrease of the slope as a function of doping was highest at a doping concentration around $1\times10^{18}/cm^3$. As an example, the difference in slopes between samples doped at 1×10^{16} and $3\times10^{17}/cm^3$ is about 0.07 eV; the difference between 5×10^{18} and $1\times10^{19}/cm^3$ is about 0.03 eV; but the difference between 1×10^{18} and $5\times10^{18}/cm^3$ is 0.25 eV. The slopes of the lightly doped samples are approximately equal to the half-energy-gap value of single-crystalline silicon. Figure 5 shows hole Hall mobility as a function of $1/kT$ for four samples. For the samples doped 1×10^{18} and $5\times10^{18}/cm^3$ the experimental data yield straight lines having slopes of 0.15 and 0.0335 eV, respectively. For samples doped 1×10^{19} and $5\times10^{19}/cm^3$ the data deviate from straight lines. The mobility of the $5\times10^{19}/cm^3$ doped sample decreases as the temperature is raised, while all the other samples showed increased mobility with temperature.

THEORY

A polycrystalline material is composed of small crystallites joined together by grain boundaries. The angle between the orientations of the adjoining crystallites is often large. Inside each crystallite the atoms are arranged in a periodic manner so that it can be considered as a small single crystal. The grain boundary is a complex structure, usually consisting of a few atomic layers of disordered atoms. Atoms in the grain boundary represent a transitional region between the different orientations of neighboring crystallites. There are two schools of thought concerning the effects of the grain boundary upon the electrical properties of doped polycrystalline semiconductors. One school[3] believes that the grain boundary acts as a sink for impurity atoms due to impurity segregation at the grain boundary. Consequently, the amount of impurity in the crystallite is reduced, which leads to a much smaller carrier concentration than the uniformly distributed impurity concentration. The carrier concentration does not approach that of the doping concentration until the grain boundary is saturated with impurity atoms. It was also suggested[5] that segregation of impurity caused the grain interiors to have higher resistance than the grain boundaries. However, it has been shown[7] that segregation of boron at the grain boundary is significant only at extremely heavily doped concentrations of silicon, e.g., 1.3 at.% of boron. No segregation was observed for doping as high as $1.3\times10^{20}/cm^3$.[7] If the reduction of carriers is the result of impurity segregation at the grain boundary, it is expected that the carrier concentration reduction would depend on the impurity element. It was observed[4] that both boron and phosphorus behaved similarly in polysilicon. It is also difficult to explain how impurity segregation can lead to the mobility minimum seen in Fig. 2.

The other school of thought[2,4] reasons that since the atoms at the grain boundary are disordered, there are a large number of defects due to incomplete atomic bonding. This results in the formation of trapping states. These trapping states are capable of trapping carriers and thereby immobilizing them. This reduces the number of free carriers available for electrical conduction. After trapping the mobile carriers the traps become electrically charged, creating a potential energy barrier which impedes the motion of carriers from one crystallite to another, thereby reducing their mobility. Based on this model, for the same amount of doping, the mobility and carrier concentration of a polycrystalline semiconductor would be less than that of a single-crystalline material. Kamins[4] used this model to explain some of the trends observed in his Hall-effect data. He attributed the decrease in mobility with decreasing carrier concentration to the effect of the high-resistivity space-charge region surrounding the grain

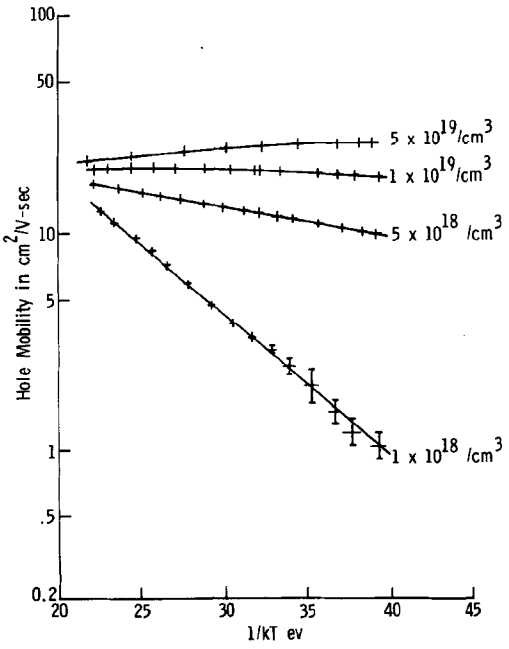

FIG. 5. Hole Hall mobility vs $1/kT$ for samples with different doping concentrations.

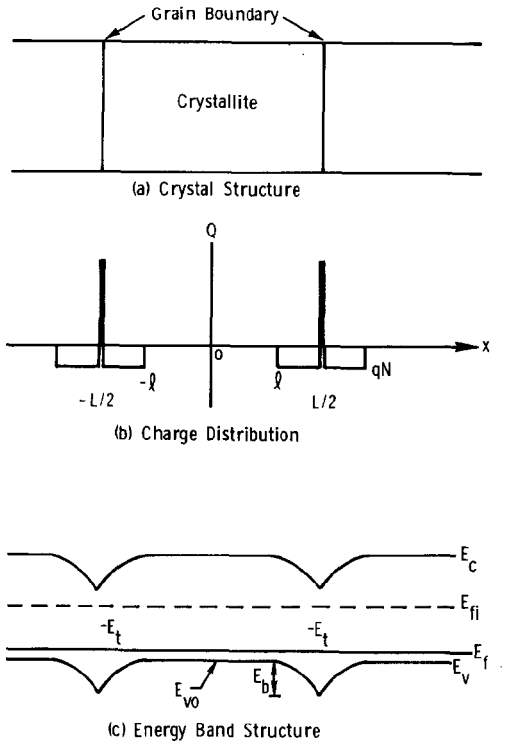

FIG. 6. (a) Model for the crystal structure of polysilicon films. (b) The charge distribution within the crystallite and at the grain boundary. (c) The energy band structure for polysilicon crystallites.

boundary. Choudhury and Hower[2] used the same model and treated the potential energy barrier as a parameter to explain their measurements of resistivity vs doping concentration.

We believe that the electrical transport properties of polysilicon films are governed by carrier trapping at the grain boundary. In a real polycrystalline material, the crystallites have a distribution of sizes and irregular shapes. To simplify the model we assume that polysilicon is composed of identical crystallites having a grain size of L cm. We also assume that there is only one type of impurity atom present, the impurity atoms are totally ionized, and uniformly distributed with a concentration of N/cm^3. The single-crystalline silicon energy band structure is also assumed to be applicable inside the crystallites. We further assume that the grain boundary is of negligible thickness compared to L and contains Q_t/cm^2 of traps located at energy E_t with respect to the intrinsic Fermi level. The traps are assumed to be initially neutral and become charged by trapping a carrier. Using the above assumptions an abrupt depletion approximation is used to calculate the energy band diagram in the crystallites. In this approximation, Fig. 6 shows that all the mobile carriers in a region of $(\frac{1}{2}L - l)$ cm from the grain boundary are trapped by the trapping states, resulting in a depletion region. The mobile carriers in the depletion region are neglected in this calculation. Although polysilicon is a three-dimensional substance, for the purpose of calculating its transport properties, it is sufficient to treat the problem in one dimension. Using the above approximation, Poisson's equation becomes

$$\frac{d^2V}{dx^2} = \frac{qN}{\epsilon}, \quad l < |x| < \tfrac{1}{2}L, \tag{1}$$

where ϵ is the dielectric permittivity of polysilicon. Integrating Eq. (1) twice and applying the boundary conditions that $V(x)$ is continuous and dV/dx is zero at $x = l$ gives

$$V(x) = (qN/2\epsilon)(x - l)^2 + V_{v0}, \quad l < |x| < \tfrac{1}{2}L, \tag{2}$$

where V_{v0} is the potential of the valence band edge at the center of the crystallite. Throughout this calculation the intrinsic Fermi level is taken to be at zero energy and energy is positive towards the valence band (the energy band diagram for holes).

For a given crystallite size, there exist two possible conditions depending on the doping concentration: (a) $LN < Q_t$, and (b) $Q_t < LN$.

We first consider the case for $LN < Q_t$. Under this condition, the crystallite is completely depleted of carriers and the traps are partially filled, so that $l = 0$ and Eq. (2) becomes

$$V(x) = V_{v0} + (qN/2\epsilon)x^2, \quad |x| \leq \tfrac{1}{2}L. \tag{3}$$

The potential barrier height, V_B, is the difference between $V(0)$ and $V(\frac{1}{2}L)$, i.e.,

$$V_B = qL^2N/8\epsilon \tag{4}$$

showing that V_B increases linearly with N. Using Boltzmann statistics, the mobile carrier concentration, $p(x)$, becomes

$$p(x) = N_v \exp\{-[qV(x) - E_f]/kT\}, \tag{5}$$

where N_v is the density of states and E_f is the Fermi level. The average carrier concentration, P_a, is obtained by integrating Eq. (5) from $-\frac{1}{2}L$ to $\frac{1}{2}L$ and dividing by the grain size. The result is

$$P_a = \frac{n_i}{Lq}\left(\frac{\pi 2\epsilon kT}{N}\right)^{1/2} \exp\left(\frac{E_B + E_f}{kT}\right) \operatorname{erf}\left[\frac{qL}{2}\left(\frac{N}{2\epsilon kT}\right)^{1/2}\right], \tag{6}$$

where

$$E_B = qV_B \tag{6'}$$

and

$$n_i = N_v \exp(-\tfrac{1}{2}E_g/kT) \tag{6''}$$

is the intrinsic hole concentration of single-crystalline silicon (with band gap E_g) at temperature T.

In Eq. (6), the Fermi level is determined by equating the number of carriers trapped to the total number of trapping states occupied, given as

$$LN = \frac{Q_t}{2\exp[(E_t - E_f)/kT] + 1} \tag{7}$$

The traps are considered to be identical; each trap is capable of trapping only one hole of either spin; and there is no interaction between traps. From Eq. (7), the Fermi level is given as

$$E_f = E_t - kT \ln[\tfrac{1}{2}(Q_t/LN - 1)]. \tag{8}$$

DOCKET ALARM

Explore Litigation Insights

Docket Alarm provides insights to develop a more informed litigation strategy and the peace of mind of knowing you're on top of things.

Real-Time Litigation Alerts

Keep your litigation team up-to-date with **real-time alerts** and advanced team management tools built for the enterprise, all while greatly reducing PACER spend.

Our comprehensive service means we can handle Federal, State, and Administrative courts across the country.

Advanced Docket Research

With over 230 million records, Docket Alarm's cloud-native docket research platform finds what other services can't. Coverage includes Federal, State, plus PTAB, TTAB, ITC and NLRB decisions, all in one place.

Identify arguments that have been successful in the past with full text, pinpoint searching. Link to case law cited within any court document via Fastcase.

Analytics At Your Fingertips

Learn what happened the last time a particular judge, opposing counsel or company faced cases similar to yours.

Advanced out-of-the-box PTAB and TTAB analytics are always at your fingertips.

API

Docket Alarm offers a powerful API (application programming interface) to developers that want to integrate case filings into their apps.

LAW FIRMS
Build custom dashboards for your attorneys and clients with live data direct from the court.

Automate many repetitive legal tasks like conflict checks, document management, and marketing.

FINANCIAL INSTITUTIONS
Litigation and bankruptcy checks for companies and debtors.

E-DISCOVERY AND LEGAL VENDORS
Sync your system to PACER to automate legal marketing.